JOURNAL OF MATERIALS SCIENCE 6 (1971) 1084–1092

A Dilatometric Study of the Orthorhombic-Tetragonal Phase Transition in Barium Sodium Niobate

J. S. ABELL, K. G. BARRACLOUGH*, I. R. HARRIS
Department of Physical Metallurgy and Science of Materials, University of Birmingham, UK

A. W. VERE, B. COCKAYNE
Royal Radar Establishment, Malvern, Worcs, UK

The thermal expansion characteristics of the two known phases of barium sodium niobate have been studied using a dilatometric technique. Observation of discontinuities in the expansion curves along the three principal axes of the room temperature orthorhombic phase have been directly related to the crystallographic changes associated with the orthorhombic-tetragonal (O-T) phase transformation occurring at ~ 260°C. A comparison of the behaviour of twinned and detwinned crystals has shown that microtwinning in the O-T transition is not a mechanism essential to the transformation; it only occurs in the orthorhombic phase to relieve the large elastic strains known to arise in the tetragonal phase on cooling. An apparently anomalous behaviour recorded on one of the crystal axes emphasises the importance of push rod geometry on determining expansion behaviour by this method. A simple geometrical model has been constructed to relate the magnitude and sense of the observed discontinuities to the composition dependence of the unit cell dimensions of the two phases, and the three general cases arising are discussed with respect to the present and previously published results.

The expansion curves of all three axes showed a well defined discontinuity at a temperature corresponding to that of the ferroelectric Curie point indicating the possibility of a first order phase change at this temperature.

1. Introduction

Barium sodium niobate† is a useful opto-electronic material [1], but the crystal quality is impaired by the occurrence of twins in the orthorhombic state (mm2) which is stable at room temperature. The twinning results from the tetragonal (4 mm) to orthorhombic transition (T-O) which occurs at approximately 260°C, [2, 3]. Previous dilatometric measurements on this material have been carried out in an attempt to explain the occurrence of cracking in single crystals when cooled through the ferroelectric Curie point at 580°C (T_c), [4-6]. The purpose of the present work is to determine the expansion characteristics of single crystals of B-S-N on cycling through the T-O transition. Expansion curves have been determined on material in which the twinning has been mechanically suppressed in order to avoid the anomalies which arise from variations in the twin distribution and density. The expansion curves are interpreted in terms of a simple geometrical model of the transformation; several apparent discrepancies between this work and earlier published work [5, 6] are explained.

2. Experimental Techniques

Expansion data were recorded for two specimens of different compositions, one close to stoichiometry the second being the congruent melting composition [7]. The analysed compositions of the material from which the dilatometer specimens were cut are given in table I. The dilatometric specimens, in the form of rectangular prisms measuring approximately 3 × 5 × 5 mm,

---

*Now at the Siemens Laboratories, Munich.

†Stoichiometric formula $Ba_2NaNb_5O_{15}$ and hereafter referred to as B-S-N

© 1971 Chapman and Hall Ltd.

TABLE I Analysed compositions of the material from which the two crystals were cut. The composition of crystal 1 is close to stoichiometric while that of crystal 2 corresponds to the non-stoichiometric congruent melting composition

Crystal	Mole % Na_2O	Mole % BaO	Mole % Nb_2O_5
1	8.0	41.0	51.0
2	7.2	42.2	50.6
Error	± 0.1	± 0.3	± 0.5

were cut with the faces perpendicular to the three orthorhombic axes. The specimens were obtained from single crystals of B-S-N grown parallel to the *c*-axis by the Czochralski method. The crystals were detwinned by the method described in reference [4].

An automatic dilatometer was used to obtain the measurements at linear heating rates of 2° per min and length changes of $\pm 2 \times 10^{-5}$ mm were readily detected. The geometry of the specimen and push-rod in this system is illustrated in fig. 1. This provides essentially point contact between the crystal and the measuring system, thus avoiding the necessity of accurate alignment of the silica and crystal faces.

A control experiment on a silica specimen enabled the results to be corrected for the changes in dimension of the silica system with increasing temperature. The length changes along the three orthorhombic axes for both crystals were recorded in the temperature range 25 to 650°C and after each series of measurements in the detwinned state, the corresponding behaviour in the twinned state was recorded. The crystal was then removed from the dilatometer and detwinned before recording the changes on another axis. This procedure enabled the direct comparison of the twinned and detwinned material.

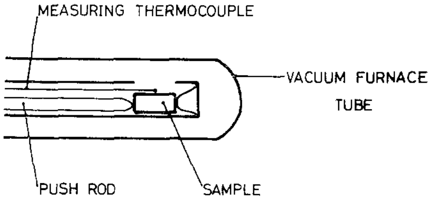

Figure 1 Schematic representation of the geometry of the push rod arrangement in the dilatometer.

The orientation of the a_0- and b_0-axes* in the crystals could not be determined by a conventional Laue method because of the very small difference in their lattice spacings (~ 0.03 Å). The axes were positively identified by conoscopic interference patterns.

3. Results

The length changes of the three principal axes of the orthorhombic cell for the two crystals are shown in figs. 2 and 3, where in each case (a) corresponds to the detwinned state and (b) the twinned state.

A comparison of the curves shown in figs. 2a and b shows that there are five features of particular interest. These can be summarised as follows:

(i) In the detwinned state (2a), the curves for the a_0- and b_0-axes diverge in the temperature range 25 to 260°C. For the twinned state (2b) the two curves are virtually coincident in this temperature range.

(ii) Small but significant expansion discontinuities were observed in all three axes in the detwinned state in the temperature range 260 to 280°C, i.e. in the region of the orthorhombic-tetragonal transition. The largest effects were observed in the a_0- and b_0-axes, which exhibited a marked increase and decrease in length respectively, in this temperature range. In contrast, no clearly observed effects were seen in these two axes in this temperature range in the twinned material.

(iii) In both the detwinned and twinned crystal, the rate of expansion of the original a_0- and b_0-axes in the temperature range 280 to 580°C, is approximately the same.

(iv) The behaviour of the *c*-axis is apparently independent of the initial state of the crystal, and in both the detwinned and twinned states the *c*-axis exhibits a small increase in the rate of expansion in the range 260 to 280°C. The most significant feature of the *c*-axis curve is the increasingly negative coefficient of thermal expansion at temperatures in the range 380 to 580°C.

(v) All three axes exhibit marked changes in slope at 580°C, i.e. at the ferroelectric Curie point, T_c. Above this temperature, the original a_0- and b_0-curves remain parallel, and the *c*-axis exhibits little change in dimension with increasing temperature up to the limit of the present measurements at 650°C.

The cooling curves of crystal 1 exhibited the

---

*The subscripts O and T refer respectively to the orthorhombic and tetragonal unit cells. In this work, the convention $b_0 > a_0$ has been adopted.

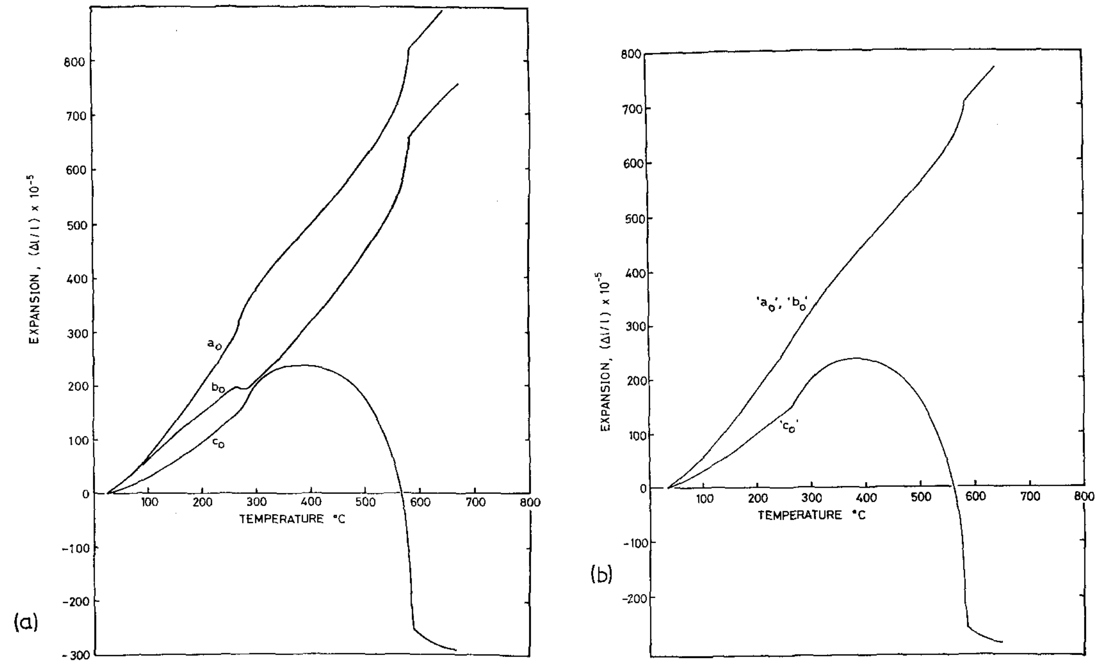

Figure 2 Expansion curves of the three orthorhombic axes of crystal 1 in the (a) detwinned and (b) twinned states. The curves are labelled with respect to the initial orthorhombic phase, the twinned state being denoted by inverted commas since a_0 and b_0 are indistinguishable. The curves of the 'a_0' and 'b_0' directions of this crystal were virtually coincident on this scale and, for clarity, only one has been shown.

same general characteristics between 650 and 280°C as that depicted in fig. 2a. However, the changes observed in the heating cycle between 260 and 280°C were far less pronounced on cooling and occurred consistently 30° lower than on the heating cycle.

The expansion characteristics of crystal 2 in the detwinned and twinned condition are illustrated in figs. 3a and b respectively. Although the general features of these curves are similar to those of crystal 1, there are important differences which can be summarised as follows:

(i) The discontinuities which correspond to the orthorhombic to tetragonal transition and the ferroelectric Curie point, occur at temperatures which are 20° lower than the previous crystal.

(ii) The difference in behaviour of the detwinned and twinned states in the 260 to 280°C region is less pronounced in this crystal.

(iii) In the twinned state, the sign of the discontinuity in the "b_0"-axis curve is contrary to expectation (cf. figs. 2b and 3b).

(iv) The cooling curve for the b_0-axis of this crystal in the twin-free state (dotted line in fig. 3a) is markedly different from that observed previously. The behaviour of this axis below the T-O transition is closely similar to that of the a_0-axis. The net result is an apparent contraction of the b_0-axis at room temperature. In general, the observed T-O effects on cooling were again less marked in this crystal and occurred ~ 10° lower than on the heating cycle. A summary of the observed temperatures for the O-T and T_C transitions on heating and cooling for the two crystals is given in table II.

TABLE II Observed temperature ranges of the orthorhombic-tetragonal transformation and the Curie point for the two crystals tested.

Crystal	T_{O-T} (°C)		T_C (°C)	
	Heating	Cooling	Heating	Cooling
1	260 to 280	230 to 250	585	580
2	240 to 260	230 to 250	565	560

Optical examination of the two crystals after each set of measurements on a particular axis consistently revealed the twin networks shown in the two micrographs in fig. 4. It should be noted that crystal 2 has a lower density and less homo-

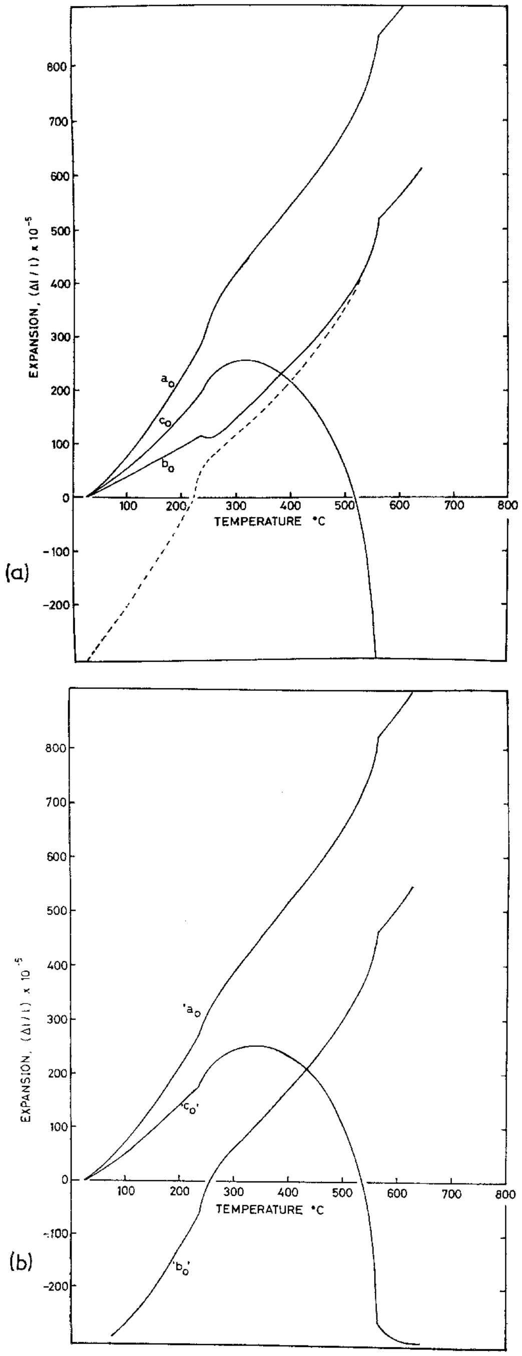

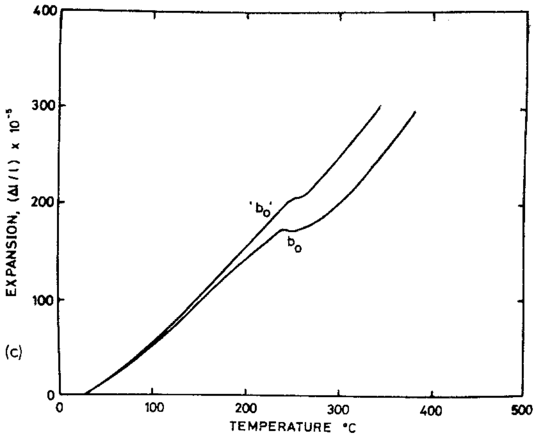

Figure 3 Expansion curves of the three orthorhombic axes of crystal 2 in the (a) detwinned and (b) twinned states. The magnitude of the c-axis contraction in (a) was slightly greater than in (b) and the whole curve could not be plotted on the present scale. However, the well-defined nature of the T_c discontinuity was still observed. Also shown in (a) is the cooling curve (dotted) corresponding to the original b_0-axis. The 'b_0' curve in (b) is the corresponding twinned state curve. (c) shows detwinned and twinned curves along the b_0-axis recorded with the flat-ended push rod.

geneous distribution of twins than crystal 1. Examination of crystal 2 *in situ*, after studying the apparently anomalous b_0-axis behaviour, showed that the position of the tip of the silica push rod on the surface of the crystal coincided with a large twin burst and this burst is shown in the optical micrograph in fig. 4.

In order to study the influence of the push rod geometry, the b_0-axis measurements on crystal 2 were repeated using a flat-ended push rod and the heating and cooling curves in the range 25 to 400° C were redetermined both in the detwinned and twinned states. In contrast to the initial measurements in this direction, the behaviour in both states is very similar (fig. 3c) and on cooling, the heating curve is essentially retraced in each case.

4. Discussion

Previous work [4] on single crystals of B-S-N has shown that the microtwinning which occurs in the orthorhombic phase as a consequence of the T-O transition, divides the crystal into a series of rectangular prisms arranged such that the b_0-axis of one is parallel to the a_0-axis of the adjacent prism, with the c-axis forming the major direction of all the prisms. This explains why it is not possible to differentiate between the expansion characteristics of the a_0- and b_0-axes on a macroscopic scale in the fully twinned, orthorhombic state, since each direction contains a_0 and b_0 components in approximately equal numbers and therefore an average reading is obtained. Hence

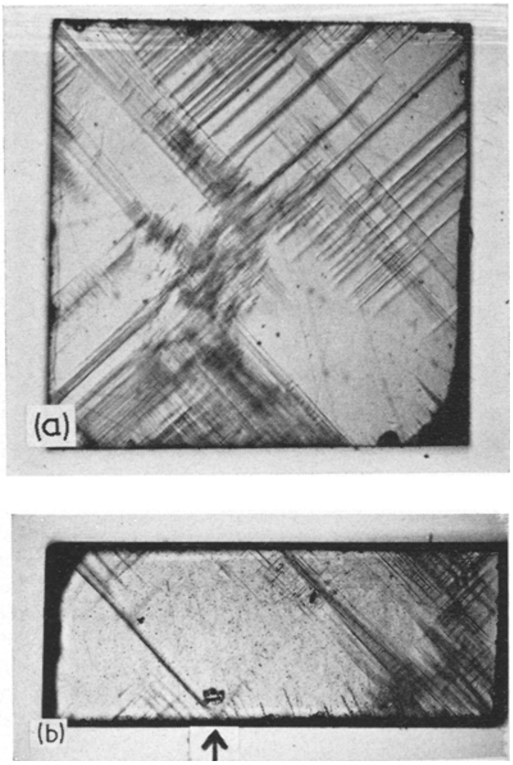

Figure 4 Optical micrographs of the twin networks in (a) crystal 1(×10) and (b) crystal 2(×8). The arrow in (b) indicates the position of the push rod tip while recording the b_0-axis expansion behaviour shown in fig. 3a.

the 'a_0'- and 'b_0'- expansion curves shown in fig. 2b are coincident over the temperature range 25 to 260°C.

In the detwinned condition, however, the different expansion characteristics of the a_0- and b_0-axes are distinguishable and the anisotropy of the orthorhombic lattice produces a small but significant divergence in the a_0- and b_0-expansion curves up to the O-T transition. This behaviour is illustrated in figs. 2a and 3a. The expansion rate of a_0 is greater than that of b_0 for both crystals which, knowing $b_0 > a_0$ at room temperature [8], implies that the orthorhombic distortion is decreasing as the O-T transition is approached. The extent of the divergence differs for the two crystals and is clearly a result of the dependence on composition of the lattice parameters of the orthorhombic phase [9, 10] within the B-S-N homogeneity range.

The dilatometric effects observed at the O-T transition indicate that only small volume changes are involved in this transformation, and this is consistent with its basic crystallography [4]. The $[110]_T$ and $[1\bar{1}0]_T$ directions of the tetragonal unit cell ($a_T \sim 12.5$ Å, $c_T \sim 4$ Å) transform respectively to the $[100]_0$ and $[010]_0$ directions of the orthorhombic unit cell with $a_0 \lesssim b_0 \sim 17.6$ Å and $c_0 \sim 4$ Å*. Thus, this transformation can be achieved by very small atomic movements since a tetragonal cell with lattice parameter $= a_T \sqrt{2} \sim 17.6$ Å can be generated from the original tetragonal unit cell by a simple rotation without any volume change, and only small displacements are then required to change this larger tetragonal cell into an orthorhombic form with the appropriate lattice dimensions. It is these small atomic displacements which are observed in the O-T transition on heating a detwinned crystal, as shown in figs. 2a and 3a. In both these cases, increases in a_0 and c_0 and a slight decrease in b_0 of the orthorhombic cell produce the tetragonal cell.

A comparison of the $\Delta l/l$ changes at the O-T transition for the twinned and detwinned states shows that, in general, the observed effects are more well-defined in the detwinned material. As already mentioned, in an ideal twinned state there are equal volumes of both orientations of crystallite and hence, in the 'a_0'- and 'b_0'-directions, the expansion in one prism is balanced by the contraction in an adjacent prism, so that the net change in length would be zero in both directions, providing $\Delta a_0 = -\Delta b_0$ at the O-T transition. Thus, in this idealised state, no change in $\Delta l/l$ would be observed on passing through the O-T transition. In practice however, there will be an inhomogeneous distribution of twins in the crystal so that the magnitude of the observed discontinuity in a particular direction will be dependent on the twin distribution in that direction, together with the relative magnitude and sign of the individual a_0 and b_0 changes at the O-T transition. Thus, in general, in the twinned material there will be an observable discontinuity at the O-T transition.

The coincidence of the 'a_0'- and 'b_0'-expansion curves for crystal 1 in the twinned condition up to O-T (fig. 2b) indicates a uniform twin distribution in this material. The slight increase in the expansion rate at the O-T transition is thought to be due to the fact that $\Delta a_0 > -\Delta b_0$ for this crystal, and this is

---

*The results of a recent X-ray investigation [12] suggest that the c-axis of the true orthorhombic unit cell is approximately double that of the unit cell referred to here.

supported by the relative magnitude of these effects in the detwinned material (fig. 2a). Crystal 2 has a lower density and less homogeneous distribution of twins (fig. 4b) and this is related to the low defect density probably associated with this congruent melting composition [7]. Consequently, the difference in the a_0- and b_0- expansion behaviour in the twinned and detwinned condition is less pronounced (figs. 3a, b and c).

If the twinning shears are confined to the (001) plane, the expansion characteristics along the $[001]_0$ direction (c-axis) should not be affected by the presence of twins in these crystals. Comparison of the c-axis behaviour in (a) and (b) of figs. 2 and 3 shows that this is indeed the case.

The magnitude and sign of the $\Delta l/l$ discontinuity at the O-T transition will depend on the relative values of the appropriate lattice spacings of the two phases at the transformation temperature. Thus, ignoring for the moment the c-axis changes at the transition, a simple two dimensional model can be proposed to explain the observed changes in a_0 and b_0. The three possible cases arising are represented in figs. 5a, b and c, together with the schematic representation of the consequent a_0 and b_0 expansion curves:

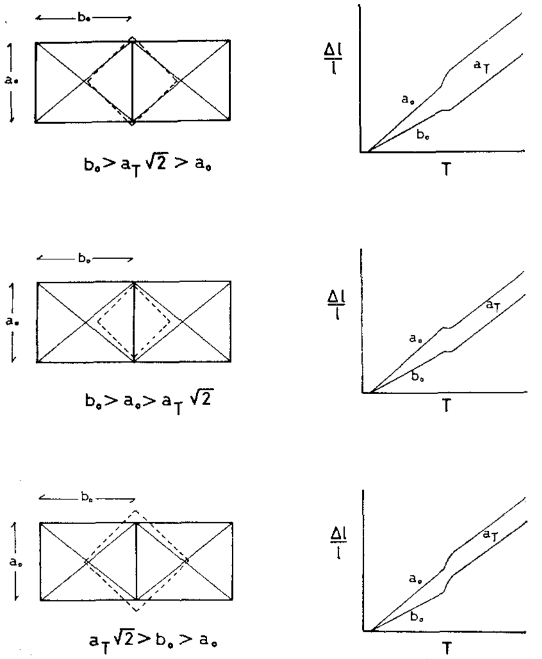

Figure 5 Schematic representation of possible two-dimensional crystallographic relationships between the orthorhombic (solid line) and tetragonal (dotted line) cells and the consequent effect on the expansion curves.

(a) In the first case $b_0 > a_T\sqrt{2} > a_0$ at T_{O-T}. At the O-T transition, b_0 must decrease and a_0 increase to achieve the correct tetragonal cell dimensions. The consequent expansion curves are shown in fig. 5a and it is clear that this is the form of the curves observed in the present work (figs. 2a and 3a). If it is assumed that the room temperature lattice parameters of crystal 1 are identical to those given by Barns [8], i.e. $a_0 = 17.591818$, $b_0 = 17.625596$ and $c_0 = 3.994915$ Å, then the expansion curves shown in fig. 2a can be used to calculate the difference between a_0 and b_0 as a function of temperature:

Temperature	$b_0 - a_0$
Room temperature	0.034
260°C	0.016
300°C	0.004

These calculations show that, even though a_0 expands more rapidly than b_0 up to the transition temperature, discontinuities of the observed sign and magnitude are required for the crystal to assume tetragonal symmetry.

(b) In the second case when $b_0 > a_0 > a_T\sqrt{2}$, at T_{O-T}, then a_0 and b_0 must decrease, giving the schematic curve shown in fig. 5b.

(c) The final possibility is $a_0 < b_0 < a_T\sqrt{2}$ at T_{O-T}, and in this case both axes must increase in the manner shown in fig. 5c.

In all three cases, the anisotropy of a_0 and b_0 will be apparent in the expansion curves up to the O-T transition (providing the crystal is detwinned). Above this transition, the expansion curves for these two axes will be parallel, reflecting the two-dimensional isotropic behaviour of the tetragonal phase.

The very simplified geometrical model presented here accounts for the effects observed in the a_0 and b_0 axes in the present work. It can also be used to explain the differences between the present work and that reported in reference [5]. In the latter work, both the a_0 and b_0 axes exhibited negative discontinuities in the 260 to 280°C temperature range and a similar result has been observed in one of the crystals examined in the authors' laboratories. The a_0 and b_0 behaviour in this case can be explained in terms of case (b) of the present model, represented in fig. 5b, i.e. $b_0 > a_0 > a_T\sqrt{2}$ and this indicates that the volume of the orthorhombic cell is larger than the tetragonal cell into which it transforms. In that work, the crystal was not detwinned before recording each expansion curve, but twinning will only tend to obscure the discontinuities associated with the transition if the a_0 and b_0 discontinuities are of the opposite sign. The latter appears to be the case in the dilatometric curves published by Vere *et al* [4] where no detwinning was performed. Behaviour corresponding to cases (*a*) and (*b*) of this model have thus been observed and there seems no apparent reason to exclude case (*c*). This clearly indicates that composition changes within the B-S-N phasefield which are known to affect the room temperature lattice parameters [9, 10], also radically affect the atomic displacements involved in the O-T transition.

These simple geometric arguments take no account of the *c*-axis behaviour at the O-T transition and a significant feature of the present work is that a *c*-axis discontinuity has been clearly observed at the O-T transition in both crystals. Jamieson *et al* [11] have shown that an ordered arrangement of the NbO_6 octahedra in B-S-N produces a doubling of the *c*-axis of the orthorhombic cell and such an effect has been reported recently in some B-S-N crystals on the basis of oscillation and rotation X-ray photographs [12]. If such an effect is occurring in the orthorhombic phase of the present crystals then this could be responsible for the *c*-axis anomaly at the O-T transition. The magnitude of the *c*-axis is particularly sensitive to the composition, in particular the Nb_2O_5 content [9] and it may be that, only for those compositions for which case (*a*) of the present model is appropriate, do the associated atomic movements require a slight expansion of the *c*-axis at the O-T transition. This probably explains the absence of *c*-axis discontinuities at the O-T transition in the previous expansion work on B-S-N crystals [5, 6] although an effect might be implied from the expansion curves of Vere *et al* [4].

An alternative explanation of the *c*-axis discontinuity is that the *c*-axes of the crystals examined in the present work were off orientation so that components of the discontinuities associated with the a_0 and b_0 axes would be detected. In the present work however, neither crystal was more than 2° off orientation and it is unlikely that such a small misorientation would give rise to such a marked effect. In addition, the magnitude of this discontinuity would then be affected by the presence of twins in the crystal and this does not appear to be the case. It would appear, therefore, that the *c*-axis discontinuity represents an increase in the *c*-spacing at the O-T transition for these crystal compositions, but the exact nature of this transformation will only be fully resolved when the compositional dependence of the a_0-, b_0-and c_0-effects at the O-T transition has been studied.

The present experiments indicate that twinning acts as a strain-relieving mechanism rather than as a transformation mechanism. Previous work [4] has shown that on cooling (001) slices of B-S-N below T_c, a diffuse pattern appears which is attributable to elastic strain within the crystal lattice and this pattern becomes increasingly distinct as the cooling continues. It is these elastic instabilities, particularly associated with the $[1\,1\,0]_T$ and $[1\,\bar{1}\,0]_T$ directions, which are thought to be responsible for the T-O transition [13]. Not until a temperature of 240° C is microtwinning observed in these crystal slices, implying that the associated strains are not relieved until transformation to the O-phase has been achieved. These twins disappear again on reheating above the transition temperature range, but it is clear from the well-defined nature of the O-T transition exhibited by detwinned material in the present experiments that twinning is not necessary for the transformation to proceed. Further evidence of this is provided by microscopic examination of a detwinned crystal heated through the transition; only elastic strains are observed when the crystal has transformed to the tetragonal phase. The crystals used in the present work were grown parallel to the *c*-axis and in those cases the twins are nucleated at the defects parallel to the *c*-axis which provide local stress concentrations having components on the $(1\,1\,0)_0$ and $(1\,\bar{1}\,0)_0$ twin planes. This stress concentration increases as the temperature falls and eventually exceeds the twinning stress. Clearly, the resultant room temperature twin density depends directly upon the underlying defect density.

Incidental evidence of twinning occurring at localised stress concentrations is provided by the anomalous b_0-axis behaviour in crystal 2. As already mentioned, the low twin density observed in this crystal (fig. 4b) is probably related to the low defect density associated with the invariant composition, [7]. In the absence of other suitable nucleation sites, it is concluded that the twin burst coinciding with the tip of the push rod was nucleated by the stress concentration at the point of contact. The required stress is supplied by the spring loaded armature of the measuring transducer. The sharp contraction observed in this direction is thus due to the macroscopic shear associated with the twin burst. The twinned region is then orientated such that its a_O-axis is parallel to the direction of measurement and the subsequent contraction rate reflects this, the curve being approximately parallel to the a_O heating curve. On reheating this crystal, the typical a_O characteristics are repeated (fig. 3b). A true macroscopic measurement of the twinned state of this crystal was only obtained by substituting a flat push rod in the system when that particular twin burst did not occur. This result emphasises the importance of the push rod geometry in dilatometric measurements. This is especially true in materials exhibiting inhomogeneous behaviour such as oxides, where twinning often accompanies transformation; significantly different and possibly misleading interpretations of specimen behaviour from microscopic and macroscopic measurements are thus possible.

It is well established that the microtwinning can be satisfactorily suppressed by cooling through the T-O transition with a suitable compressive stress applied along $[110]_T$ or $[1\bar{1}0]_T$ direction. The result is a twin free crystal with the shorter a_O-axis of the orthorhombic cell aligned parallel to the compression axis. This experimentally observed fact enables a positive identification of the associated twin shear directions to be made; this is illustrated in fig. 6 where the planes and directions are referred to the orthorhombic phase. Suppression of twin formation by the compressive stress indicated by the bold arrows, along a direction which becomes $[100]_O$ leads to the conclusion that the twin shears on the $(110)_O$ and $(1\bar{1}0)_O$ habit planes are in the directions shown, since the shears are confined to the (001) planes. Thus, the operative twin systems are $(110)_O$ $[1\bar{1}0]_O$ and $(1\bar{1}0)_O$ $[110]_O$. The anomalous b-axis behaviour of crystal 2 is consistent with this result since the direction of the applied push rod stress, along the $[010]_O$ direction, is now seen to favour twin formation.

The nature of the curves in the region of T_c suggest that the ferroelectric-paraelectric transition is accompanied by a structural transformation. The parallel behaviour of the two a_T axes both immediately below and above T_c indicate that tetragonal symmetry is retained, but the c-axis behaviour indicates a significant decrease in the c/a ratio. Although gradual changes in the tetragonal parameters occur prior to the Curie temperature, particularly in the c-axis, the discontinuity in the curves at T_c is in each case very well-defined. This indication of a first order effect is in marked contrast to other c-axis expansion data where this transition was of a more diffuse nature [5, 6]. It is hoped that the precise nature of the structural change occurring at T_c and its dependence on composition within the B-S-N phase field will be resolved by high temperature X-ray diffraction experiments currently being undertaken.

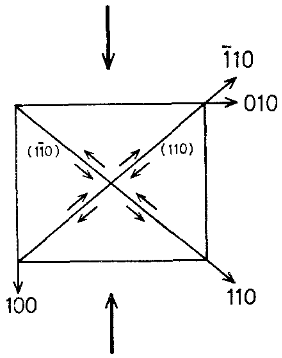

Figure 6 Analysis of the twinning shears in the (001) plane of the orthorhombic unit cell. The bold arrows represent the direction of the compressive stress which suppresses twin formation.

Acknowledgements

This paper is published by permission of the Copyright Controller, HMSO. The authors wish to thank Professor R. E. Smallman for the provision of some of the laboratory facilities.

References

1. J. J. RUBIN, L. G. VAN UITERT, and H. J. LEVENSTEIN, *J. Cryst. Growth* **1** (1967) 315.
2. J. E. GEUSIC, H. J. LEVENSTEIN, J. J. RUBIN, S. SINGH, and L. G. VAN UITERT, *Appl. Phys. Lett.* **11** (1967) 269.
3. L. G. VAN UITERT, H. J. LEVENSTEIN, J. J. RUBIN, C. D. CAPIO, E. F. DEARBORN, and W. A. BONNER, *Mat. Res. Bull.* **3** (1968) 47.
4. A. W. VERE, J. G. PLANT, B. COCKAYNE, K. G. BARRACLOUGH, and I. R. HARRIS, *J. Mater. Sci.* **4** (1969) 1075.
5. A. A. BALLMAN, J. R. CARRUTHERS, and H. M. O'BRYAN, *J. Cryst. Growth* **6** (1970) 184.
6. W. A. BONNER, J. R. CARRUTHERS, and H. M. O'BRYAN, *Mat. Res. Bull.* **5** (1970) 243.
7. K. G. BARRACLOUGH, I. R. HARRIS, B. COCKAYNE, J. G. PLANT, and A. W. VERE, *J. Mater. Sci.* **5** (1970) 389.
8. R. L. BARNS, *J. Appl. Cryst.* **1** (1968) 290.

9. J. R. CARRUTHERS and M. GRASSO, *Mat. Res. Bull.* **4** (1969) 413.
10. B. A. SCOTT, E. A. GIESS, and D. F. O'KANE, *ibid* **4** (1969) 107.
11. P. B. JAMIESON, S. C. ABRAHAMS, and J. L. BERNSTEIN, *J. Chem. Phys.* **50** (1969) 4352.
12. L. C. BOBB, I. LEFKOWITZ, and L. MULDAWER, *J. Appl. Cryst.* **2** (1969) 189.
13. T. YAMADA, H. IWASAKI, and N. NIIZEKI, *J. Appl. Phys.* **41** (1970) 4141.

Received 20 April and accepted 4 May 1971.